IEEE Journal of Microwaves

Received 16 March 2023; revised 24 May 2023; accepted 6 August 2023. Date of publication 1 September 2023; date of current version 9 October 2023.

Digital Object Identifier 10.1109/JMW.2023.3305180

Lightweight, High-Q and High Temperature Stability Microwave Cavity Resonators Using Carbon-Fiber Reinforced Silicon-Carbide Ceramic Composite

LU QIAN [1] (Graduate Student Member, IEEE), YESHODHARA BASKARAN[2], MATTHIAS KRÖDEL[2], CÉSAR MIQUEL ESPAÑA [3], LAURENT PAMBAGUIAN[3], TALAL SKAIK [1], AND YI WANG [1] (Senior Member, IEEE)

(Regular Paper)

[1]EDT Laboratory, School of Engineering, University of Birmingham, B15 2TT Birmingham, U.K.
[2]ECM Engineered Ceramic Material GmbH, 85452 Moosinning, Germany
[3]European Space Agency, 2201 Noordwijk, AZ, Netherlands

CORRESPONDING AUTHOR: Yi Wang (e-mail: Y.Wang.1@bham.ac.uk).

This work was supported by the GSTP Program in the frame of the ESA Contract 4000131423/20/NL/FE Next Generation Temperature Compensated High Power Filters Based on Novel Materials.

ABSTRACT This article for the first time presents a high-Q cavity resonator manufactured using carbon-fiber reinforced silicon carbide (SiC) ceramic composite material HB-Cesic. This composite has attractive properties of low coefficient of thermal expansion comparable to Invar, low density similar to aluminum, and high thermal conductivity. Its manufacturing process enabled by machining and joining renders useful design flexibility. A high-Q spherical resonator has been used as an example in this investigation. Two resonators, one monolithic version and the other one based on split-block structure have been experimented. The end-to-end processes from machining, assembly or joining, to high-conductivity coating for both structures, have been demonstrated. The RF performance of the resonators and their variation with temperature have been measured. A quality factor of over 10000 has been achieved for both resonators at 11.483 GHz. The measured high thermal stability of the resonator correlates very well with the prediction. This work establishes the feasibility of using HB-Cesic in microwave resonators and paves the way for further development and verification programme for more complex passive microwave devices such as filters and multiplexers for space applications.

INDEX TERMS High-power microwave, invar alloy, novel materials, silicon carbide, space technology, spherical resonators, thermal stability.

I. INTRODUCTION

The development of satellite communication technology, especially the advent of high-throughput-satellite (HTS) systems has spurred increasing demand for high-performance microwave devices [1]. Among them, output multiplexers (OMUXs) are one of the most complex and specialized passive components. An OMUX usually consists of a set of narrowband output filters and is placed after high-power amplifier to combine multiple amplified signals into a common transmission antenna. As a result, the low insertion loss and high power-handling capacity are key design parameters. Additionally, OMUXs requires very stable RF performance over a wide temperature range. Both the self-heating effect induced by power dissipation and the operating temperature range pose significant challenge to maintaining good thermal stability of the overall filter [2], [3]. Therefore, the high quality-factor (Q) and high temperature-stability filters are a crucial component for satellite communication systems.

To achieve the low insertion-loss, high-Q resonators are needed. Many cavity resonators have been invented, such as the TE_{011} single mode cylinder resonator, TE_{11N} (N = 1 - 5) and TE_{221} dual-mode cylinder resonators [4]. Enabled by the emerging additive manufacture (AM) technology, some irregular shaped resonators, such as super-ellipsoid and spherical cavity resonator, were also reported [5], [6], [7], [8], [9], [10], [11].

For the stringent thermal stability requirement, two methods have been widely adopted. The first method relies on the temperature-invariant material like Invar, which has very low coefficient of thermal expansion (CTE) of 1-2 ppm/K [12]. However, its poor manufacturability due to hardness, high density, and low thermal conductivity are significant barriers to their widespread application, particularly as more microwave components are required in emerging satellite internet constellation systems. The second method uses external temperature compensation [13], [14]. Often external fixture or additional compensation structures are required. This can complicate the assembly. A lot of the compensation fixtures are made from Invar. To address the manufacturability issue with Invar, 3-D printing has been used to manufacture Invar filter and diplexer [15], [16], [17]. Recently, we have reported some investigative work on using novel low-CTE alloy materials to manufacture thermally stable microwave components [18]. However, so far none of the metal materials can match the low CTE of Invar.

Non-metal materials that can match the CTE of Invar are some ceramic based materials and carbon-fibre-reinforced polymers (CFRPs). CFRP is an interesting material for high power applications. It has low density, high specific stiffness and a very low CTE down to $-0.4 \sim 0.76$ ppm/K. However, its anisotropic properties often complicate the microwave design. This material has been used in antennas for space applications, as well as in circuit packaging. One major challenge with this material is the metal coating. CFRP is conductive but has a very low conductivity. CFRPs have been reported for filters applications [19]. One other high-power filter based on a similar material was originally reported in 1974 [20] and reviewed in 2016 [21]. The material used was Graphite Fiber Epoxy Composite (GFEC), with a CTE similar to Invar but a ∼50% weight reduction. The work also highlighted the anisotropic issue of the material and consequentially the restriction on the design.

Silicon carbide (SiC) is a family of compound semiconductor consisting of silicon and carbon. Because of its unique crystalline structures, SiC has excellent physical properties such as high electric field breakdown strength, high maximum current density, and high thermal conductivity. It has been used in electronic industry including power electronics [22], photonics [23] and is regarded as a promising substrate for high-temperature quantum devices [24]. Carbon-fiber reinforced silicon carbide is a ceramic composite material. This material has high hardness and stiffness, high thermal conductivity, and low coefficient of thermal expansion. It also overcomes the anisotropic issue with CFRP, capable of producing uniform and isotropic structures. HB-Cesic is such a material developed by ECM - Engineered Ceramic Material GmbH [25]. Its low CTE, light weight and high thermal conductivity offer almost a perfect combination for high temperature-stability microwave components. Table 1 summarises the comparison of the thermal and mechanical property between HB-Cesic and Invar alloy as well as the aluminum alloy (A20X).

TABLE 1. Mechanical and Thermal Properties

Mechanical & Thermal Properties	HB-Cesic® [25]	Invar [15]	A20X [18]
Density (g/cm^3)	2.96	8.1	2.85
Young's modulus (GPa)	350	140	75
CTE (ppm/K)	2.3	0.5-2	20.4
Thermal Conductivity (W/(m·K))	200	15	175

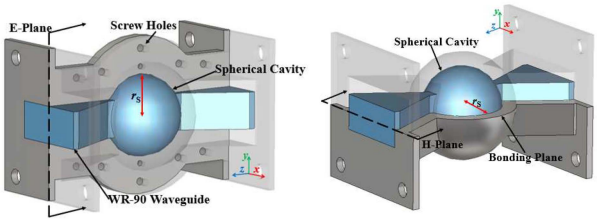

(a) (b)

FIGURE 1. Configuration of two spherical resonators, where half of the metallic wall is rendered with translucent colour to aid visualization. The blue colour represents the air cavity. (a) Split-block resonator, (b) monolithic resonator.

This work, for the first time, investigated the feasibility of HB-Cesic in microwave passive components. The manufacturing process for microwave components will be explored. Both the material itself and the manufacturing processes are a novelty for the microwave community. A spherical resonator has been used as an example in this investigation. Compared with rectangular cavity resonators, the spherical resonators have higher quality factor and wider spurious-free window, while the curved surface presents a demanding test structure to verify the feasibility of the proposed manufacturing approach. Two resonators, one based on a single-piece (monolithic) build and the other on a two-piece (split-block) structure, have been experimented. The end-to-end manufacturing process has been demonstrated. Experimental characterization is performed to investigate the RF performance and thermal stability. The measurement result exhibits a good correlation with the theoretical prediction.

II. SPHERICAL RESONATOR

Fig. 1 illustrates the configuration of the spherical resonator, where both the monolithic and the split-block version are shown. The resonator consists of a spherical cavity and two WR-90 waveguide ports. The dominant mode TM_{101}, resonating at 11.483 GHz, is weakly coupled through the narrow coupling iris. The unloaded quality-factor (Q_u) value is

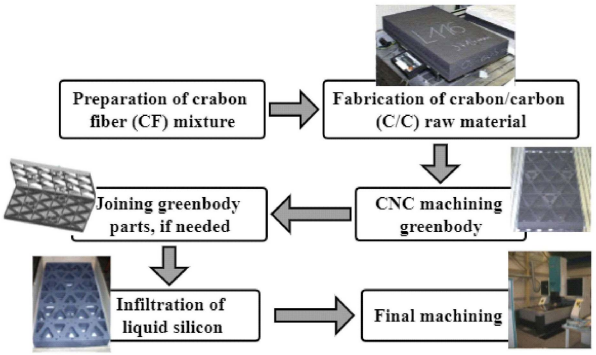

FIGURE 2. Flowchart of the manufacturing process of HB-Cesic parts.

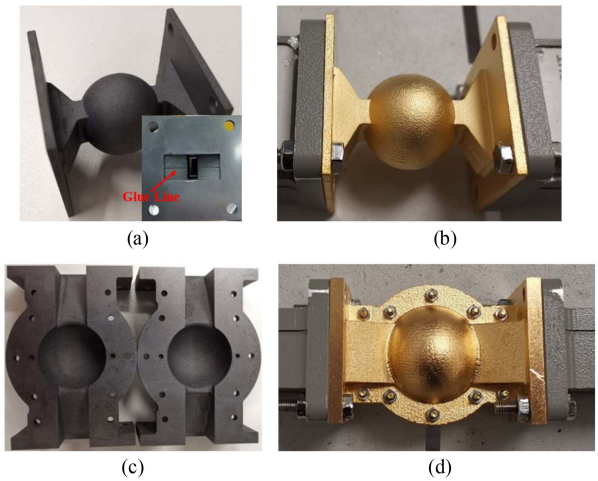

FIGURE 3. Photograph of the two HB-Cesic resonators. (a) Monolithic resonator (before coating), (b) monolithic resonator (after coating), (c) split-block resonator (before plating). (d) split-block resonator (after plating).

calculated to be 11075, assuming the conductivity of perfectly smooth gold (4.56×10^7 S/m).

For the split-block spherical resonator (see Fig.1(a)), the resonator is formed of two identical parts that are bolted together, along the E-plane of the rectangular waveguide port to reduce the disturbance to the surface current and therefore its sensitivity to assembly. Fig. 1(b) shows the monolithic spherical resonator. It should be noted that it was glued together from two identical parts along the H-plane. In this structure, H-plane is not normally the preferred cut. However, the bonding technique used for the HB-Cesic material promises to eliminate the usual problem associate with imperfect contacts between two parts. This monolithic resonator structure serves to test the robustness of the manufacture technology, which will be discussed in more detail later.

III. FABRICATION

Fig. 2 presents the flowchart outlining the manufacturing process of HB-Cesic parts. The process is divided into several sequential steps, as follows: (1) Preparation of carbon fiber (CF) mixtures. In this step, CF will be mixed with resin and other carbon powders. (2) Fabrication of carbon/carbon (C/C) raw material. The C/C raw material is formed by pressing CF mixtures to a solid block. (3) CNC machining the C/C blocks to form the desired structure (greenbody) using diamond tools. (4) Liquid silicon infiltration. The greenbody parts are infiltrated by liquid silicon and then fired at high-temperature furnace to form the final HB-Cesic parts. (5) Final machining of interfaces or functional surfaces. The manufacturing process offers several advantages over conventional ceramic materials. For instance, the C/C greenbody is not fragile, allowing for the production of very thin walls and the creation of ribs with a diameter of 1 mm and height of 100 mm. The infiltration is a solid-to-solid process resulting in no shrinkage. Consequently, it helps to mitigate geometry inaccuracies caused by sintering. Furthermore, the manufacturing process facilitates the formation of complex monolithic closed structures by joining separately machined greenbody parts using glues prior to silicon infiltration. The joining technology uses a non-commercial adhesive, which has a very similar microstructure as the C/C material. At the stage of applying, the adhesive is a pasty material and curing will get hard. In the following high temperature process the adhesive will be converted with silicon to the same material as the bulk C/C material showing no difference in mechanical and thermal properties. Micrographic analysis also indicates no discontinuity in the joining area.

HB-Cesic has a very low electrical conductivity of 28.7 S/m. So, metal coating is imperative. This material has been used in antenna reflectors [26]. Copper coating was applied by magnetron sputtering on the open structures. For the closed structures like the resonator, there is no established coating process reported in the open literature. We have experimented and applied electroless copper plating to both the open structure split-block and the closed monolithic resonator. The measured RF performance (discussed in the next section) has indicated full coverage and good quality of the coating. The electroless process is limited in achievable thickness. Only 1 - 2 mm coating was achieved. This has been thickened up by electroplating copper and passivated with a thin gold finishing. The as-fired surface roughness of HB-Cesic parts is typically less than 8 μm. This is higher than CNC machined surface, but comparable to 3D printed metal surfaces. For the two resonators, the measured average surface roughness before and after plating is 2.1 μm and 1.7 μm. The measured RF performance again indicates the impact on the losses is not significant for the X-band resonator. Fig. 3 shows the pictures of both HB-Cesic spherical resonators, as-manufactured and after gold plating respectively. The wall thickness of both resonators is 4 mm except that the flange thickness of the monolithic resonator is reduced to 2 mm.

IV. MEASUREMENT AND DISCUSSION

To validate the material and manufacturing technology for high-power microwave components, both RF and thermal-RF tests were carried out.

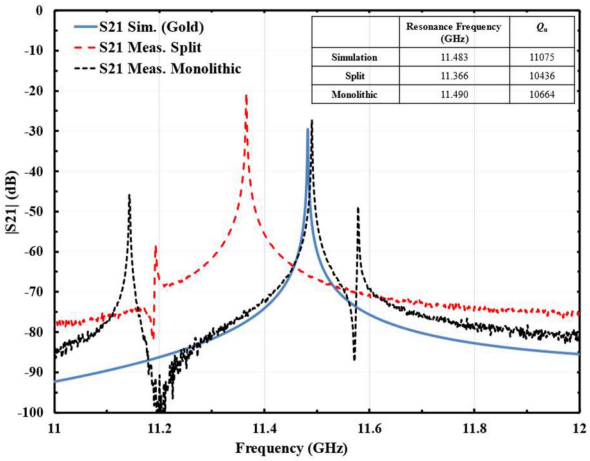

	Resonance Frequency (GHz)	Q_u
Simulation	11.483	11075
Split	11.366	10436
Monolithic	11.490	10664

FIGURE 4. Measured and simulated result of the two resonators with inset showing the comparison of resonance frequency and Q_u.

A. RF MEASUREMENT

All RF measurements were performed on Agilent E8361C PNA network analyser. The analyser was calibrated using TRL (Thru, Reflect, Line) method. To achieve accurate Q measurements, the intermediate frequency of the sweep was set to be 100 Hz. Fig. 4 shows the measured and simulated transmission response (S_{21}) of the resonators. The measured Q_u, extracted using 3-dB method, of the monolithic resonator is 10664. This is 10436 for the split-block resonator. Both values are very close to the simulated Q_u of 11075 based on a perfect conductivity of gold. This means the hybrid plating techniques can achieve very good electrical conductivity. This also indicates the assembly plane of the split-block resonator has very small impact on Q_u. It should be noted that the Q extracted using 3-dB method is practically the loaded quality-factor (Q_L), but it nearly equals to Q_u for the very weakly coupled resonators. To improve the accuracy of the extraction, the bandwidth of the frequency sweep is limited to only 3 to 5 times of the 3-dB bandwidth. For the split resonator, the resonance frequency is shifted downward by 117 MHz to 11.336 GHz. There is a spurious spike at 11.2 GHz. For the monolithic resonator, the resonance only shifts slightly up by 7 MHz. Two spurious spikes appear at 11.2 GHz and 11.58 GHz. Because the spherical resonator supports three degenerate modes and high-order modes, the spurious spikes are mostly likely a result of geometry deviation that breaks the symmetry and excites the unwanted modes. This has been investigated using simulation analyses next.

Fig. 5 presents the main results from this investigation where several possible manufacturing and assembling errors were considered. For the split-block resonator, we first look at the displacement between the two halves as shown in Fig. 5(a), along the Y-axis (denoted by d_Y), while the spherical radius r_S is increased from 11.34 mm to 11.425 mm to account for the frequency shift. It is clear the intended resonance frequencies agree well after this modification, while

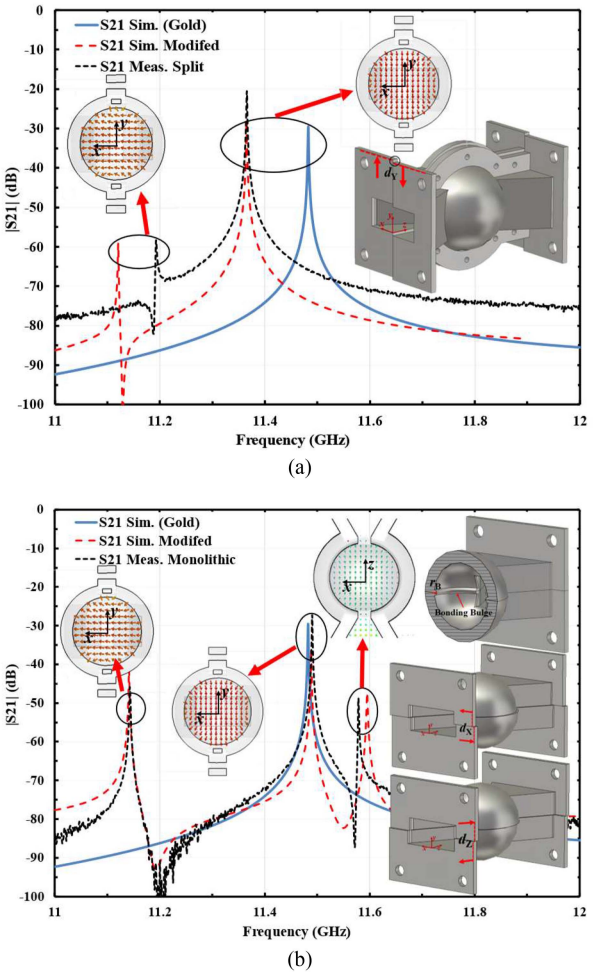

FIGURE 5. Comparison between the measured and simulated transmission responses with inset showing the modified resonator model considering the manufacturing and assembling errors, and the simulated E-field cross-section at the resonator centre. (a) Split resonator, $d_Y = 0.05$ mm. (b) Monolithic resonator, $r_B = 0.85$ mm, $d_X = 0.09$ mm, and $d_Z = 0.17$ mm.

a spurious spike can be observed in the lower band. The simulated Electric-field (E-field) distribution at the resonance and the spike frequency are presented in the inset. It shows the dominant and the spurious mode correspond to the degenerate TM_{101} mode. The small frequency difference between the simulated and measured spikes might be caused by other asymmetries of the spherical resonator such as the unequal radius along X-axis or Y-axis. It is expected the spurious spikes can be mitigated by reducing the displacement d_Y during assembly.

For the monolithic resonator, three possible cases are considered. As illustrated in the inset of Fig. 5(b), the first is a bulge along the bonding plane (denoted by r_B) from the glue line as shown in the inset of Fig. 2(a). The other two are the displacement along X-axis (d_x) and Z-axis (d_z). The simulation responses from the modified resonator model shows an excellent consistency with the measurement results. According to simulation analysis, the slight upper shift of the intended resonance frequency is mainly caused by the

TABLE 2. Comparison of the HB-Cesic and Invar Resonators

	Weight (g)	Q_U (R.T. / 85°C)	Freq. temp. coefficient (ppm/K)
Monolithic Cesic	31	10664 / 10131	1.77
Split-block Cesic	45	10436 / 9483	2.36
3-D Printed Invar	117	7995 / 7454	1.01

R.T.: room temperature.

bonding bulge (r_B). Looking at the simulated E-field pattern, we can find the lower spike is derived from the degenerate TM_{101} mode due to the displacement in *X*-axis while the higher spike resembles the degenerate TM_{101} mode due to the displacement in *Z*-axis. It is expected these spurious modes can be suppressed by improving the accuracy of the joining and eliminating the glue line. Changing the bonding plane to the E-plane could also reduce the risk of spurious spikes.

B. TEMPERATURE-DEPENDENT RF MEASUREMENT

To verify the thermal stability of the HB-Cesic microwave components, the temperature-dependent RF measurement was performed. The experiment process is similar to that in [18]. However, as shown in Fig. 6(a), a 3D-printed Invar waveguide spacer was inserted between the HB-Cesic resonator and the aluminium test port to mitigate the thermal stress that could be induced by the mismatched CTE of the ceramic part and aluminium ports. Fig. 6(b) presents the comparison of measured effective temperature coefficient (ETC) [17] between the two resonators, where the inset is the measured transmission responses as a function of temperature for both resonators. The ETC is calculated using the frequency shift and temperature interval between two consecutive temperature points. During the measurement, 5 MHz frequency-sweep bandwidth is applied to all temperature points to ensure accuracy of the extracted resonance frequency. Both resonators show good thermal stability (ETC $<$ 3 ppm/K) up to 80 °C, the typical maximum operating temperature of common OMUXs. The ETC of the monolithic resonator is less than 2 ppm/K. These results are comparable to the measured CTE of 2.3 ppm/K of the bulk Cesic material. The monolithic resonator has an ETC below 3 ppm/K up to 160 °C. The ETC of the split-block resonator is higher and rises to 6 ppm/K at 160 °C. The considerable increase of its ETC above 100 °C is believed to be attributed to the aluminium screws used to bolt the two halves. This effect may be reduced by using Invar or Cesic screws. Fig. 6(c) shows the variation of Q_u versus the temperature. A decreasing trend can be observed, but the Q_u is still great than 9000 up to 160 °C for both resonators. This still leaves adequate design margin for the channelizing filters in OMUXs, where the desired Q_u is usually around 6000.

For comparison, a 3-D printed Invar spherical resonator with identical internal dimensions and 2 mm wall thickness was manufactured and measured. The Invar resonator was plated with silver. Table 2 summarises the comparison. The HB-Cesic resonators exhibit a clear advantage in terms of the weight and the achievable Q_u. The monolithic resonator

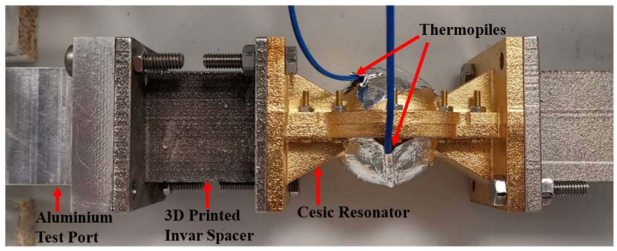

(a)

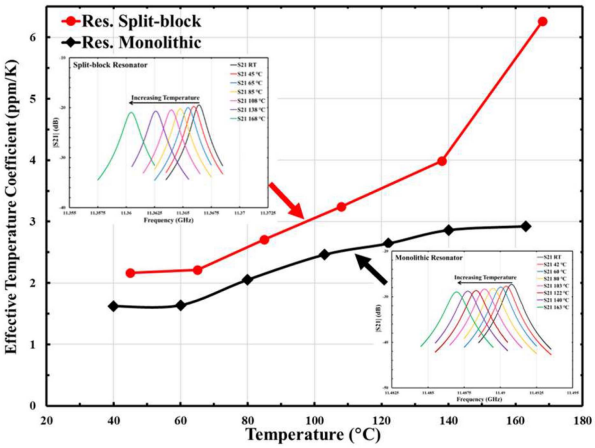

(b)

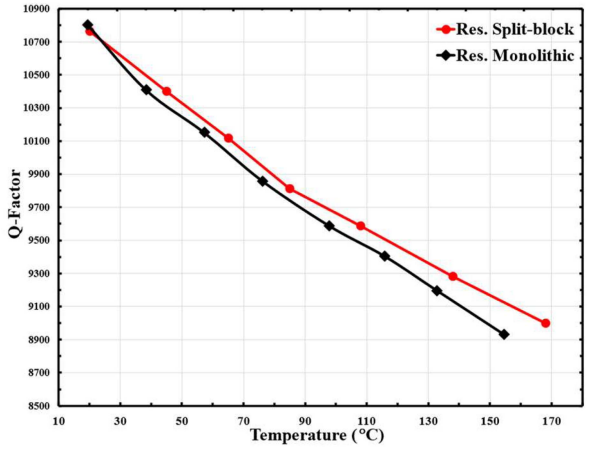

(c)

FIGURE 6. Thermal-RF measurement results as a function of temperature. (a) Resonator under test; (b) effective temperature coefficient with inset showing the measured transmission responses at different temperatures for both resonators; (c) unloaded quality factor (Q_u).

realizes 74% mass reduction while achieving 39% increase in Q_u. Even in the case of the split resonator, the improvements in weight and Q_u are 62% and 31%, respectively. Considering the thermal stability, we find that the HB-Cesic resonators can achieve slightly higher ETC values than Invar resonator. These values are still competitively low and can be used to meet the typical thermal-stability requirement for high-power devices like OMUXs.

TABLE 3. A Comparison With Published High-Q Spherical Resonators

Ref.	Resonator Type	Resonance Mode	f_c (GHz)	Q_u (Sim./Meas.)	Manufacture Technology	Material
[7]	Spherical resonator	TM_{101} (Dominant Mode)	10	14450/-	3-D Printing	Polymer (Copper plating)
[8]	Squeezed spherical resonator	TM_{101} (Dominant Mode)	10	6820/3728	3-D Printing	Al-Cu alloy
[5]	Depressed super-ellipsoid resonator	TM_{101} (Dominant Mode)	12.875	6102/4300	3-D Printing	Scalmalloy aluminium alloy
[9]	Spherical resonator	TM_{211} (Higher-order Mode)	31	7393/493	3-D Printing	AlSi10Mg alloy
[10]	Spherical resonator	TE_{101} (Higher-order Mode)	10	23000/4500	3-D Printing	AlSi10Mg alloy
[11]	Spherical resonator	TE_{101} (Higher-order Mode)	10	23000/1200	3-D Printing	Polymer (Copper plating)
[17]	Spherical resonator	TM_{101} (Dominant Mode)	11.483	12500/5800	3-D Printing	Invar alloy (Silver plating)
T.W.	Spherical resonator	TM_{101} (Dominant Mode)	11.483	11075/10664 11075/10436	CNC	HB-Cesic® (Gold plating)

Ref: reference, f_c: central frequency, Q_u: unloaded quality-factor; CNC: computer numerical control; T. W.: this work.

Table 3 provides a comparison with published high-Q spherical resonators. As can be observed, the HB-Cesic spherical resonators achieve the highest Q_u among all measurement results. While higher-order resonance modes could potentially achieve even higher Q_u than the dominant mode used in this work, spurious modes nearby would limit their practical application, particularly when wide stopband is required. Moreover, the novel HB-Cesic material not only improves thermal stability but also reduces weight compared with Invar and many other metallic materials.

V. CONCLUSION

A lightweight, high-Q and high temperature stability spherical resonator manufactured from HB-Cesic composite has been reported. To the best of authors' knowledge, this is the first SiC-ceramic-based microwave resonator reported in the open literature. The material properties and end-to-end manufacturing approach are introduced. Detailed experimental characterization and verification have been performed. The causes for the frequency discrepancy and spurious spikes have been analysed. The former is mainly caused by spherical radius variation whereas the latter is due to the discontinuity introduced by the assembly errors and the glue line. It is expected these spurious modes can be mitigated by optimising the manufacture process, increasing assemble accuracy and choosing appropriate bonding plane. The advantage of the HB-Cesic resonators in Q_u and weight reduction have been demonstrated. Both resonators achieved the Q_u of over 10000 and 60% mass reduction, while achieving comparable thermal stability to Invar resonator. This work confirms the feasibility of using HB-Cesic in microwave resonators and provide a new technology for highly thermal-stable microwave devices, paving the way for further development and verification programme for more complex passive microwave devices such as filters and multiplexers for space applications.

REFERENCES

[1] Y. Vasavada, R. Gopal, C. Ravishankar, G. Zakaria, and N. BenAmmar, "Architectures for next generation high throughput satellite systems," *Int. J. Satell. Commun. Netw.*, vol. 34, no. 4, pp. 523–546, 2016.

[2] P. Martin-Iglesias, M. V. D. Vorst, J. Gumpinger, and T. Ghidini, "ESA's recent developments in the field of 3D-printed RF/microwave hardware," in *Proc. 11th Eur. Conf. Antennas Propag.*, 2017, pp. 553–557.

[3] F. De Paolis and C. Ernst, "Challenges in the design of next generation ka-band OMUX for space applications," in *Proc. 31st AIAA Int. Commun. Satell. Syst. Conf.*, 2013, pp. 1–7.

[4] R. J. Cameron, C. M. Kudsia, and R. R. Mansour, *Microwave Filters for Communication Systems*. Hoboken, NJ, USA: Wiley, 2018.

[5] P. Booth and E. V. Lluch, "Enhancing the performance of waveguide filters using additive manufacturing," *Proc. IEEE*, vol. 105, no. 4, pp. 613–619, Apr. 2017.

[6] F. Zhang et al., "3-D printed slotted spherical resonator bandpass filters with spurious suppression," *IEEE Access*, vol. 7, pp. 128026–128034, 2019.

[7] C. Guo, X. Shang, M. J. Lancaster, and J. Xu, "A 3-D printed lightweight x-band waveguide filter based on spherical resonators," *IEEE Microw. Wireless Compon. Lett.*, vol. 25, no. 7, pp. 442–444, Jul. 2015.

[8] C. Guo et al., "Shaping and slotting high-Q spherical resonators for suppression of higher order modes," in *IEEE MTT-S Int. Microw. Symp. Dig.*, 2019, pp. 1205–1208.

[9] F. Zhang, G. Torregrosa-Penalva, E. Àvila-Navarro, N. Delmonte, L. Silvestri, and M. Bozzi, "A 3-D printed bandpass filter using TM-mode slotted spherical resonators with enhanced spurious suppression," *IEEE Access*, vol. 8, pp. 213215–213223, 2020.

[10] E. Lopez-Oliver et al., "Very high Q-factor bandpass filter using additive manufacturing," in *Proc. IEEE MTT-S Int. Microw. Filter Workshop*, 2021, pp. 243–245.

[11] E. Lopez-Oliver and C. Tomassoni, "Stereolithography additive manufacturing of overmoded spherical filters," in *Proc. Microw. Mediterranean Symp.*, 2022, pp. 1–4.

[12] B. Yassini and M. Yu, "Ka-band dual-mode super Q filters and multiplexers," *IEEE Trans. Microw. Theory Techn.*, vol. 63, no. 10, pp. 3391–3397, Oct. 2015.

[13] B. L. Steven, "Temperature compensated microwave filter," U.S. Patent US5867077A, 1999.

[14] F. William, M. Yu, D. Smith, and A. Sivadas, "Microwave resonator having an external temperature compensator," U.S. Patent 6535087B1, Aug. 18, 2003.

[15] C. Qiu, N. J. E. Adkins, and M. M. Attallah, "Selective laser melting of Invar 36: Microstructure and properties," *Acta Mater.*, vol. 103, pp. 382–395, 2016.

[16] X. Wen et al., "An invar alloy SLM printed diplexer with high thermal stability," *IEEE Trans. Circuits Syst. II, Exp. Briefs*, vol. 69, no. 3, pp. 1019–1023, Mar. 2022.

[17] L. Qian et al., "A narrowband 3-D printed invar spherical dual-mode filter with high thermal stability for OMUXs," *IEEE Trans. Microw. Theory Techn.*, vol. 70, no. 4, pp. 2165–2173, Apr. 2022.

[18] L. Qian et al., "Thermal stability analysis of 3D printed resonators using novel materials," in *Proc. IEEE 51st Eur. Microw. Conf.*, 2022, pp. 334–337.

[19] S. Liberatoscioli, M. Mattes, M. Guglielmi, D. Schmitt, and C. Ernst, "Innovative manufacturing technology for RF passive devices combining electroforming and CFRP application," in *IEEE MTT-S Int. Microw. Symp. Dig.*, 2008, pp. 743–746.

[20] C. M. Kudsia and M. V. O'Donovan, "A light weight graphite fiber epoxy composite (GFEC) waveguide multiplexer for satellite application," in *Proc. 4th Eur. Microw. Conf.*, 1974, pp. 585–589.
[21] C. Kudsia, T. Stajcer, and M. Yu, "Evolution of microwave technologies for communications satellite systems," in *Proc. 34th AIAA Int. Commun. Satell. Syst. Conf.*, 2016, Art. no. 5739.
[22] C. R. Eddy and D. K. Gaskill, "Silicon carbide as a platform for power electronics," *Science*, vol. 324, no. 5933, pp. 1398–1400, Jun. 2009.
[23] D. M. Lukin et al., "4H-silicon-carbide-on-insulator for integrated quantum and nonlinear photonics," *Nature Photon.*, vol. 14, no. 5, pp. 330–334, May 2020.
[24] F. Reis et al., "Bismuthene on a SiC substrate: A candidate for a high-temperature quantum spin hall material," *Science*, vol. 357, no. 6348, pp. 287–290, Jul. 2017.
[25] "HB-cesic data sheet," Mar. 2019. [Online]. Available: https://www.cesic.de/galerie
[26] P. Noschese, M. Herbellau, A. T. Fossdal, and R. Harper, "X/Ka high temperature high gain antenna for the mission bepi colombo to the planet mercury," in *Proc. Eur. Conf. Antennas Propag.*, 2006, Art. no. 685.

LU QIAN (Graduate Student Member, IEEE) was born in Hunan, China. He received the B.Eng. degree (Hons.) in information engineering and the M.S. degree in information and communication system from the South China University of Technology, Guangzhou, China, in 2016 and 2019, respectively. He is currently working toward the Ph.D. degree in electronic engineering with the University of Birmingham, Birmingham, U.K.

His research interests include microwave filters, multiport coupled-resonator network, and 3-D printed microwave devices.

YESHODHARA BASKARAN, photograph and biography not available at the time of publication.

MATTHIAS KRÖDEL, photograph and biography not available at the time of publication.

CÉSAR MIQUEL-ESPAÑA was born in València, Spain. He received the Licenciado degree (Hons.) in physics and the Ph.D. degree in theoretical physics from the Universitat de València, Valencia, Spain, in 2002 and 2008, respectively.

He is currently with the European Space Agency as the Deputy Director of the High Power RF and Space Materials Laboratories. His research interests include microwave filters, ferrite devices, additive manufacturing, and high power RF phenomena.

LAURENT PAMBAGUIAN received the Ph.D. degree in mechanical behaviour of interfaces in metal matrix composites from ONERA, The French Aeronautic Lab, in 1994. He did two post docs in Spain on heterogeneous deformation of aluminium alloys and in Austria on metal matrix composites. In 1999, he has been recruited as the Engineer of Materials and Processes Section of the European Space Agency and focussed on addressing the development of advanced materials and processes for the future ESA missions. Since 2004, he has been the first to develop Additive Manufacturing Technologies at ESA and is expanding his expertise on this topic.

TALAL SKAIK received the M.Sc. degree in communications engineering and the Ph.D. degree in microwave engineering from the University of Birmingham, Birmingham, U.K., in 2007 and 2011, respectively.

After Ph.D, he worked in lecturing in electrical engineering untill 2019. He is currently a Research Fellow with the Electronic, Electrical and Systems Engineering Department, University of Birmingham. He has authored or coauthored more than 30 refereed research papers. He acts as a reviewer of various microwave journals and for the European Microwave Conference. His research interests include millimeter-wave and terahertz filters and antennas, 3D-printed microwave devices, temperature compensated filters for satellite payloads, and multi-port coupled resonator structures.

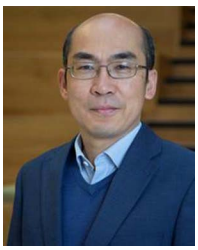

YI WANG (Senior Member IEEE) was born in Shandong, China. He received the B.Sc. degree in applied physics and the M.Sc. degree in condensed matter physics from the University of Science and Technology, Beijing, China, in 1998 and 2001, respectively, and the Ph.D. degree in electronic and electrical engineering from the University of Birmingham, Edgbaston, Birmingham, U.K., in 2005.

From 2004 to 2011, he was a Research Fellow with the University of Birmingham. In 2011, he became a Senior Lecturer and then Reader with the University of Greenwich, London, U.K. He is currently a Professor of microwave engineering with the University of Birmingham. He leads the Emerging Device Technology (EDT) Research Lab, specializing in the application of new materials and advanced manufacturing techniques to high frequency devices. He is also the Academic Lead of the Engineering Cleanroom and the Terahertz Measurement Facility at Birmingham. He is the author of more than 220 research papers and has been the Associate Editor for IET MAP. He was the TPC Chair of 2021 European Microwave Conference. His research interests include 3D printed microwave and mm-wave devices, waveguide antenna technology, multiport filtering networks, filter-antenna integration, millimeter-wave and sub-terahertz antennas and devices for metrology, communication, and sensing. He is particularly interested in working with new materials and novel manufacturing techniques for RF/microwave applications.